ELSEVIER

Thermochimica Acta 388 (2002) 27–40

thermochimica acta

www.elsevier.com/locate/tca

Role of the mutual contamination in the synergetic effects between MoO_3 and SnO_2

E.M. Gaigneaux[a,*,1], S.R.G. Carrazán[b], P. Ruiz[a], B. Delmon[a]

[a]*Unité de catalyse et chimie des matériaux divisés, Université catholique de Louvain, Croix du Sud 2/17, B-1348 Louvain-la-Neuve, Belgium*

[b]*Instituto de Química, Facultad de Química, Universidad de Salamanca, Salamanca, Spain*

Received 23 July 2001; received in revised form 28 November 2001; accepted 28 November 2001

Abstract

This contribution is an answer to the criticism that the synergetic effects observed between SnO_2 and MoO_3 in the catalytic dehydration–dehydrogenation of 2-butanol to butene (BUT) and methyl–ethyl–ketone (MEK), in the presence of oxygen and at low temperature (463 K), are not due to a remote control mechanism via the migration of spillover oxygen (Oso) but to the formation of a more active and selective mutual contamination of the oxides during catalysis. Experiments especially designed to artificially induce different types of mutual contamination between SnO_2 and MoO_3 and then to evaluate their catalytic performances have been conducted. Three types of contaminated samples were synthesized: Mo ions deposited at the surface of SnO_2, a solid solution of Mo in SnO_2 lattice and a Sn–Mo–O mixed oxide precursor. The contaminated samples were tested alone and in the presence of SnO_2 and MoO_3. The conclusion is that, for reasons of unstability and/or of low performance, none of the mutual contamination compounds investigated can account for the synergetic effects between SnO_2 and MoO_3. Other experiments conducted with SnO_2 and MoO_3 in the selective oxidation of isobutene at high temperature (693 K) confirm the existence of a synergism between the oxides. In this case, SnO_2 is very active, which induces its continuous reduction during the reaction. To maintain its initial high oxidation level, SnO_2 pumps lattice oxygen from MoO_3. The consequence is that MoO_3 turns progressively reduced. It is shown that an additional supply of Oso succeeds to prevent this phenomenon. Finally, more specific experiments lead to a better understanding of the mechanism by which active sites are formed under the action of Oso. Oso is formed at the surface SnO_2 (which is an Oso donor). It then migrates onto the surface of MoO_3 (which is an Oso acceptor) where it increases the acidity, and thus the dehydration activity, of MoO_3. This accounts for the synergetic increase of the production of BUT observed for mechanical mixtures of SnO_2 and MoO_3.

Keywords: 2-Butanol; Butene (BUT); Spillover oxygen (Oso)

1. Introduction

Synergetic effects between MoO_3 and SnO_2 have been previously observed in the catalytic dehydration–dehydrogenation of 2-butanol carried out in the presence of oxygen and at low temperature (423–473 K). Yields and selectivities in butene (BUT) and methyl–ethyl–ketone (MEK) obtained for mixtures of SnO_2 and MoO_3, synthesized separately and thereafter gently contacted together mechanically, were indeed higher than those obtained for the pure oxides used individually under identical conditions of catalytic reaction [1]. Similar results were obtained in the same reaction

* Corresponding author. Fax: +32-10-47-36-49.
E-mail address: gaigneaux@cata.ucl.ac.be (E.M. Gaigneaux).

[1] Chercheur qualifié research associate for the 'Fonds National de la Recherche Scientifique (FNRS) of Belgium.

0040-6031/02/$ – see front matter
PII: S0040-6031(02)00050-3

carried out with mechanical mixtures of MoO_3 and α-Sb_2O_4. For this system, the proposed interpretation was that the improved reactivity of MoO_3 is due to a remote control mechanism between oxide phases remaining totally separate [2]. The remote control mechanism considers that α-Sb_2O_4 behaves as a spillover oxygen (Oso) donor, i.e. that it is able to activate O_2 to monoatomic mobile Oso species. These Oso species migrate onto the surface of MoO_3 with which they react, so inducing the creation and the regeneration of the oxidation and dehydration catalytic sites. The consequence of the mechanism is thus an improvement of the performance of MoO_3 when it is used as catalyst in the presence of α-Sb_2O_4. The remote control mechanism has been proposed to explain several cases of synergetic effects in oxidation processes on multiphase oxide catalysts—in this case Oso species are involved, but also in hydrodesulfurization processes on multiphase sulfur catalysts—in this case spillover hydrogen species are involved [3–5].

Recent works have allowed to further progress in the understanding of the exact role of Oso at the surface of Oso acceptor phases. In the selective oxidation of isobutene, a synergetic effect was observed between MoO_3 and α-Sb_2O_4, corresponding to an enhanced production of methacrolein. In this system, it was shown that Oso, produced by α-Sb_2O_4, induces the dynamic reconstruction of the (0 1 0) basal faces of MoO_3 crystals to nanometric (1 0 0) facets and pits with some walls oriented as (1 0 0). As (1 0 0) faces are more active and selective in oxidation processes than the basal faces, this accounts for the higher performance of MoO_3 in the presence of α-Sb_2O_4 [6,7]. The same reconstruction was observed when MoO_3 crystals were used in the presence of α-Sb_2O_4 as catalyst for the oxygen-assisted dehydration of 2-butanol [8,9].

Another aspect of the role played by Oso at the surface of Oso acceptor concerns the stabilization of the active metals in a higher oxidation state under the conditions of reaction. The phenomenon was clearly observed in the case of the use of MoO_3 in the dehydration of 2-butanol [8,9]. In this reaction, MoO_3, used alone, underwent a deep reduction of its surface to MoO_2. The reduction was accompanied by a violent fragmentation of the MoO_3 crystals. Deep reduction and fragmentation did not happen when MoO_3 was used in mechanical mixture with α-Sb_2O_4, but, on the contrary, the surface of MoO_3 was stabilized during the reaction to a MoO_{3-x} suboxide stoichiometry. On one hand, MoO_2 proved to be less active in the dehydration of 2-butanol than Mo oxides with higher oxidation states. On the other hand, MoO_{3-x} suboxides are characterized by crystallographic shear structures allowing easy oxygen exchanges with the gas phase, which confers them a high activity as oxidation catalysts. The difference of behavior for MoO_3 in the presence and in the absence of Oso thus accounted for the synergetic improvement of performance induced when MoO_3 was used in mixtures with α-Sb_2O_4. The ability of Oso to maintain the surface of oxides in a higher oxidation state during oxidation reactions was also observed in the case of Bi molybdates used as catalysts in the oxidative dehydrogenation of 2-butanol [10]. The implications of the effects of Oso, and the promising perspectives to use Oso and the remote control mechanism as efficient tools to improve the catalytic performance of oxides in oxidation processes have been pointed in a recent short review [11].

In the case of the synergetic effects between MoO_3 and SnO_2 in the dehydration–dehydrogenation of 2-butanol, the suggested interpretation of the enhanced performance of MoO_3 is that SnO_2 acts as an Oso donor, so indirectly improving the activity of MoO_3, which behaves as an Oso acceptor [2]. Inspite of the fact that SnO_2 has already been checked to be an efficient Oso donor [12], the classical criticism arisen against this interpretation is that the synergetic effects could also be explained by a minute mutual contamination between MoO_3 and SnO_2 or by the formation of a new mixed Sn–Mo–O phase occurring under the conditions of reaction from the starting pure oxides mixed together mechanically. The criticism rests on the unchecked hypothesis that such mutual contamination compound or mixed oxide phase could be more active and selective than the pure Sn and Mo oxides.

The present work corresponds to an answer to this criticism. We report experiments intentionally planned to study in depth the origin of the synergetic effects between SnO_2 and MoO_3 in the dehydration–dehydrogenation of 2-butanol in the presence of oxygen. In particular, it was investigated whether the synergetic effects could be explained by the formation of possibly more active and selective mutual

contamination between the two oxides. Three types of contaminated samples were prepared. In a first part, we have artificially contaminated SnO_2 by depositing on its surface, via an impregnation method, different concentrations of Mo ions. A comparative study of the theoretical and the experimental XPS signals has been made in order to study the stability of the contaminating impregnated ions and to evaluate their tendency to form crystallites or to remain as well dispersed monolayers at the surface of SnO_2. The catalytic performances of the samples were thereafter measured in the dehydration–dehydrogenation of 2-butanol. The role of the artificial contamination was evaluated at the light of the characterization results obtained for the samples before and after the catalytic reaction. Additional experiments aimed at studying the influence of such impregnated layer of Mo ions on the activity of pure oxides. Therefore, one of the impregnated samples was used as catalyst in mixtures with pure SnO_2 and pure MoO_3.

In a second part, another artificially contaminated sample was prepared in a way attempting to maximize the chance to form a solid solution of Mo in SnO_2. It is speculated that a solid solution could form from a thin layer of Mo oxide at the surface of SnO_2 maintained under typical conditions of catalysis during a long time. The solid solution sample was thus prepared by submitting one of the impregnated samples to the 2-butanol reaction. The sample was thereafter mixed with the pure oxides and tested again in the reaction.

The third part aimed at studying the catalytic behavior of an oxide compound associating Sn and Mo in the bulk. The ''citrate method'' was used for the synthesis as it proved to be particularly adequate to prepare mixed oxide phases [13]. The method consists in preparing an amorphous precursor in which both metals of the desired mixed phase, here Mo and Sn, are homogeneously dispersed in a citrate complex. It is thereafter attempted to form the mixed oxide by carefully burning the precursor. A study of the stability of a possible Sn–Mo–O phase was realized as a function of the temperature of burning. Mixtures of the Sn–Mo–O samples with pure oxides were prepared and the catalytic performances were measured.

Additional explanations about the role of Oso and the way by which it brings about the synergetic effects are given on the basis of temperature programmed ammonia desorption experiments. Finally, a further exploration of the synergetic effects between SnO_2 was done with the oxidation of isobutene to methacrolein at high temperature (693 K) as the probe reaction.

2. Experimental

2.1. Catalysts preparation

2.1.1. Pure oxides

Tin(IV) oxide was synthesized by dissolving $SnCl_2{\cdot}2H_2O$ (Merck, p.a.) in distilled water. The initial suspension was acidified with concentrated HCl (Janssen Chimica, p.a.) until a transparent solution was obtained. Precipitation was then realized by adding an aqueous solution of NH_3 (25%, Janssen Chimica) until pH 7 is reached. Chloride anions were thereafter washed out of the resulting tin hydroxide using the ammonia solution and distilled water. The washed solid was next put in suspension in distilled water and the water was evaporated under reduced pressure in a rotavapor at 318 K before being dried at 383 K for 20 h and then burnt in air at 873 K for 8 h and at 1173 K for 16 h. The obtained sample is hereafter denoted as SnO_2. A special tin(IV) oxide sample has additionally been prepared following the same procedure but without burning at 1173 K. This sample is hereafter denoted as SnO_2(I).

Mo(VI) oxide was prepared by dissolving equivalent quantities of $(NH_4)_6Mo_7O_{24}{\cdot}4H_2O$ (Janssen Chimica, p.a.) and oxalic acid (Janssen Chimica, p.a.) in distilled water. The initial turbid suspension was stirred at 313 K until a clear solution was obtained. The solvent was then evaporated under reduced pressure at 318 K in a rotavapor before the obtained solid was dried at 353 K for 20 h, decomposed at 573 K for 20 h and burnt in air at 673 K for 20 h. The sample is denoted as MoO_3. A special batch of Mo(VI) oxide has additionally been prepared by burning $(NH_4)_6Mo_7O_{24}{\cdot}4H_2O$ at 773 K for 20 h. This sample is denoted as MoO_3(I).

The samples prepared as described above have been checked by X-ray diffraction (XRD) to be cassiterite and molybdite [14]. Specific surface areas were, for SnO_2 and MoO_3, 3.7 and 6.3 $m^2\,g^{-1}$, respectively and for SnO_2(I) and MoO_3(I), 12.6 and 2.6 $m^2\,g^{-1}$, respectively.

2.1.2. Contaminated samples

2.1.2.1. Impregnation of SnO_2 with Mo ions. An attempt to artificially contaminate SnO_2 has been realized by impregnating its surface with Mo ions. The smallest unit in MoO_3 corresponding to the projection of a MoO_6^{6-} octahedron is 0.17 nm^2 [15]. The procedure to deposit 2 theoretical monolayers of MoO_3 on the surface of SnO_2 was as follows: 1.5 g of SnO_2 was added to an aqueous solution containing 1.66 g of $(NH_4)_6Mo_7O_{24}{\cdot}4H_2O$ in 250 ml of distilled water. The suspension was submitted to ultrasounds for 10 min and stirred for 3 h. Water was then evaporated under reduced pressure at 318 K in a rotavapor. The solid obtained was thereafter dried for 12 h at 383 K and burnt for 2 h at 673 K. Samples corresponding to 0.25, 0.5, 0.75 and 1 theoretical monolayer of MoO_3 were also prepared following the same procedure with adapted proportions. These samples are denoted as $Sn_iMo(X)$ where X corresponds to the number of theoretical monolayers of Mo deposited.

2.1.2.2. Preparation of mixed Sn–Mo–O phases. An attempt to prepare a Sn–Mo–O mixed oxide was performed as follows. $(NH_4)_6Mo_7O_{24}{\cdot}4H_2O$ was complexed with an equivalent amount of citric acid (Merck, p.a.) in distilled water. The same was achieved with $SnCl_2{\cdot}2H_2O$. Volumes of these solutions adjusted to get a Sn to Mo molar ratio of 0.5 were mixed together. The resulting dark blue solution was stirred overnight at room temperature, and then concentrated under vacuum at 303 K. The obtained viscous residue was maintained at 383 K for 20 h under 50 mbar. The solid precursor was manually ground and separated into three parts. Each part was, respectively burnt for 8 h at 723 K (sample Sn–Mo–O/723), 823 K (sample Sn–Mo–O/823) and 973 K (sample Sn–Mo–O/973) and washed with distilled water in order to remove chloride anions. Detailed XRD showed that burning the precursor at 723 K led to an amorphous solid, while burning at higher temperatures provoked a rapid crystallization of pure SnO_2 and MoO_3 [1].

2.1.2.3. Solid solution of Mo in SnO_2. An attempt to prepare a solid solution of Mo ions in SnO_2 was made by submitting the sample $Sn_iMo(0.5)$ for 4 h to the conditions of reaction used to run the dehydration–dehydrogenation of 2-butanol as described below. The obtained sample is hereafter denoted as $Sn_iMo(0.5)$ (treated).

2.1.3. Preparation of mechanical mixtures

Mechanical mixtures of the samples prepared as described above were prepared by dipping together the concerned samples in *n*-pentane. Interdispersion of the samples was achieved by stirring the suspension for 10 min and then by submitting it to ultrasounds for 10 min. Thereafter, *n*-pentane was evaporated under reduced pressure in a rotavapor at 298 K. The solid was thereafter dried in air at 353 K overnight. No additional thermal treatment was carried out. Mechanical mixtures associating pure SnO_2 with MoO_3, and each of the contamination compounds with either SnO_2 or MoO_3 were prepared. Proportions of the compounds in the different mechanical mixtures are indicated at the appropriate places in the text.

2.2. Catalytic reactions

2.2.1. Dehydration–dehydrogenation of 2-butanol in the presence of oxygen

The dehydration–dehydrogenation of 2-butanol to BUT and MEK, respectively, was performed in the presence of oxygen. The reaction was carried out in a fixed bed microreactor made of pyrex and with an internal diameter of 8 mm. The partial pressure of 2-butanol was fixed at 176 mmHg in a 90 ml min^{-1} flow of air. A mass of 500 mg of catalyst was used for each test. Catalysts were used as pellets made of compacted powder. The pellets had a granulometry between 500 and 800 μm. Under standard conditions, the catalytic activity was measured at 463 K for 3 h. Analysis of reactants and products at the reactor outlet was performed by on-line gas chromatography.

2.2.2. Oxidation of isobutene to methacrolein

The catalytic oxidation of isobutene to methacrolein was performed in a fixed bed microreactor made of pyrex and with an internal diameter of 8 mm. The catalyst was used as pellets prepared as described above. A mass of 160 mg of catalyst was used for each test. The reaction was run with a partial pressure of isobutene of 76 mmHg, a partial pressure of oxygen of 152 mmHg and partial pressure of nitrogen of 532 mmHg. The total gas flow was 30 ml min^{-1}, corresponding to a contact time of 0.5 s. The catalytic

activity was measured at 693 K. Analysis of reactants and products at the reactor outlet was performed by on-line gas chromatography.

2.3. Characterization

XRD was performed on a Kristalloflex Siemens D5000 diffractometer using the Kα radiation of Cu ($\lambda = 1.5418$ Å) between 2θ angles going from 2 to 90°. Scan rate was fixed at 0.6° min^{-1}.

Specific surface areas were measured on a Micromeritics Flowsorb II on the basis of the quantity of N_2 adsorbed at the surface of the samples at 77 K.

X-ray photoelectron spectroscopy (XPS) analyses were carried out on a VG MKII spectrometer with an Mg anode (Mg Kα = 1253.6 eV). Contamination carbon C 1s peak, taken as a reference for the measurement of kinetic energies, was set at 284.8 eV. The C 1s, Mo 3d, Sn 3d and O 1s bands were particularly investigated. The different elements were quantified using the Wagner sensibility factors. For the samples $Sn_iMo(X)$ prepared by impregnation, in order to obtain information about the support effect on the dispersion of MoO_3 at the surface of SnO_2, the observed XPS intensity ratios were examined and compared with those calculated, hereafter noted R_{th}, using the stacking monolayer model of Defossé [16]. R_{th} calculated by the model gives the theoretical intensity for a XPS band of an element (here, Mo 3d) that should be observed in the case that this element is monoatomically dispersed on the surface of the support (here, SnO_2) forming monolayers. R_{th} is given by the relation $R_{th} = adq$, where $a = R'_A R'_L R'_\sigma / C_{Sn}\lambda_{Sn}$. In this equation, $R'_A = \phi_a/\phi_b$ [17] with ϕ being the anisotropy parameter, $R'_L = L_a/L_b$, where L is the analyzer luminosity calculated using the algorithm given by Weng et al. [18] and $R'_\sigma = \sigma_a/\sigma_b$, being the cross sections taken from Scofield tables [19]. Index 'a' corresponds to Mo 3d peak and index 'b' to Sn 3d peak in the last three equations. Values of the parameters used in the calculation are given in Table 1. The volumetric atomic concentration of Sn in SnO_2, $C_{Sn} = 13.97$ atoms nm^{-3}, was calculated taking into account the formula number of SnO_2 in the unit cell ($Z = 2$) and the unit cell volume. These data were obtained from the ICDD-JCPDS file N° 211250 [14]. λ_{Sn} is the electron free path (1.283 nm) determined using the algorithm given Szajman et al. [20]. The density value of 5.51 g cm^{-3} of SnO_2 as calculated using the formula, $r = ZM/AV$, where M and A are the molecular weight of SnO_2 and the Avogadro number, respectively. Z and V are defined above. Parameter d is the surface density defined as $d = n_{Mo}/SBET$, with n_{Mo} being the number of Mo atoms per g of catalyst and SBET the surface area of the support (SnO_2) expressed in nm^2 g^{-1}. Finally, q is a factor that depends only of the SBET and turns close to 1 for low surface areas, as it does in the case of our catalysts. The observed XPS intensity ratios are calculated from $R_{exp} = I_{Mo\,3d}/I_{Sn\,3d}$ where I is the peak intensity calculated from the relation, $I =$ peak area × sensitivity factor. Taking into account parameters both depending on the sample and on the instrument, one can estimate the incertitude on this type of value around 10%.When comparing R_{th} and R_{exp}, two situations can be distinguished. Similar values for R_{th} and R_{exp} indicate that the dispersion of Mo ions at the surface of SnO_2 follows a regular staking monolayer model. But if R_{th} is higher than R_{exp}, this indicates that the impregnated Mo ions tend to sinter and to form small crystallites on the surface of SnO_2. This also means that the tendency of the system is to drastically minimize the initial artificial contamination of the impregnated samples.

Table 1
Values of the parameters ϕ, L and σ used to run the stacking monolayer model of Defossé [16]

Peak	ϕ	L	σ
Mo $3d_{5/2}$	1.297	18.378	5.77
Sn $3d_{5/2}$	1.295	21.778	14.63

A Bruker RFS100 spectrometer was used for the Raman analyses. The power of the Nd–YAG excitation laser was tuned at 15 mW in order to avoid thermal radiation, fluorescence and degradation of the samples as much as possible.

Temperature programmed desorption of ammonia (NH_3-TPD) was realized as follows: 200 mg of the sample in powder was evacuated under a 30 ml min^{-1} flow of He at 723 K for 1 h. The sample was then cooled down to room temperature in He, before He was replaced by NH_3. Adsorption was carried out for 30 min. Desorption was realized under He from room temperature up to 723 K at a rate of 10 °C min^{-1}. A catharometer (TCD) detector was used to quantify the desorbed ammonia.

3. Results and discussion

3.1. Tendency to contamination between SnO_2 and MoO_3 as a Sn–Mo–O mixed oxide

The sample Sn–Mo–O/723 only exhibited the XRD diffraction peaks of SnO_2 with low intensities. This indicates that, in this sample, SnO_2 had just started to form small crystallites. At the opposite, XRD patterns of the samples Sn–Mo–O/823 and Sn–Mo–O/973 indicated that the samples were mainly constituted of MoO_3 crystallites and SnO_2 bigger crystals. More precisely, the pattern obtained for Sn–Mo–O/973 was almost identical to the pattern obtained with a mechanical mixture containing 66 wt.% of MoO_3 and 33 wt.% of SnO_2. No peaks that could indicate the presence of a mixed Sn–Mo–O phase were found.

The specific surface area of the sample Sn–Mo–O/823 is the highest of the series (24.2 $m^2\,g^{-1}$ versus 3.3 $m^2\,g^{-1}$ for Sn–Mo–O/723). The specific surface area of Sn–Mo–O/973 (5 $m^2\,g^{-1}$) was similar to that of the corresponding mechanical mixture containing 66 wt.% of MoO_3 and 33 wt.% of SnO_2, which had a specific surface of 6.0 $m^2\,g^{-1}$, meaning that the sizes of the crystallites are similar in the two samples.

XRD and specific surface area results suggest that the burning of the mixed Sn–Mo–O precursor induces the independent crystallization of SnO_2 and MoO_3. Starting from a highly amorphous precursor associating homogeneously Sn and Mo, a progressive decontamination occurs, associated to the independent formation of simple SnO_2 and MoO_3, when the temperature of burning increases. One cannot exclude that the two oxides formed by the decomposition of the amorphous precursor could be solid solutions of each other. It is in fact highly probable that it is the case. However, in the line of our objective (checking the stability of the different types of contamination), the main conclusion is that the true bulk mixed oxide precursor decomposes spontaneously under the burning conditions used in this work, and this more rapidly and deeply at higher temperatures.

The sample Sn–Mo–O/723 had the poorest crystallinity of the series of samples. Hence, for the continuation of the investigation, i.e. measuring the catalytic performance of the most contaminated Sn–Mo–O sample, alone and in mixtures with pure SnO_2 and MoO_3, Sn–Mo–O/723 must thus be selected as it is undoubtedly the one eventually containing as much contamination (either bulk or solid solution) as possible for this series of samples.

3.2. Tendency to contamination between SnO_2 and MoO_3 in the impregnated samples

Surface area values of impregnated $Sn_iMo(X)$ samples increase of about 10% with respect to pure SnO_2 (having been submitted to the impregnation procedure but without Mo ions in the impregnating solution). XRD patterns obtained for the samples $Sn_iMo(X)$ only exhibited the features typical of cassiterite SnO_2. A careful characterization of the samples by Raman spectroscopy, which is a very sensitive technique to characterize surface Mo species on SnO_2, confirms that Mo ions readily detach from the surface of tin oxide to form small Mo oxide crystallites. Bands typical of bulk MoO_3 (at 157, 284, 666, 818 and 995 cm^{-1}) were indeed observed for the $Sn_iMo(X)$ samples. No additional bands or shifts were detected. SnO_2 does not possess any Raman signal.

In spite of the fact that Mo ions tend to form MoO_3 crystallites on SnO_2, rather than spreading on its surface, it can however not be completely excluded that some contamination occurs for low concentrations of Mo ions deposited on the surface of SnO_2. A more detailed information about the dispersion of MoO_3 on SnO_2 was obtained by comparing the observed XPS intensity ratios R_{exp} with the calculated R_{th}, respectively measured and calculated using the theoretical model as described in Section 2. R_{exp} and R_{th} values found for the $Sn_iMo(X)$ samples are presented in Table 2.

In all cases, even for the sample containing the lowest Mo concentration, $Sn_iMo(0.25)$, the experimental XPS values R_{exp} were lower than those corresponding

Table 2
Comparison of the XPS measured $I_{Mo\ 3d}/I_{Sn\ 3d}$ intensity ratios (R_{exp}) and those calculated using the stacking monolayer model of Defossé (R_{th}) [16]

Samples	$R_{exp} \times 100$	$R_{th} \times 100$
$Sn_iMo(0.25)$	3.4	5.0
$Sn_iMo(0.5)$	5.3	10.0
$Sn_iMo(0.75)$	5.8	15.0
$Sn_iMo(1)$	7.9	20.0
$Sn_iMo(2)$	11.0	40.0

calculated theoretically R_{th}. This remains valid despite the incertitude on the measurements as defined in Section 2.3. For the samples $Sn_iMo(1)$ and $Sn_iMo(2)$, experimental R_{exp} values were dramatically lower than the corresponding R_{th} theoretical ones. Thus, as already suggested from the Raman investigation, the XPS study strongly suggests that the impregnated Mo ions readily detach from the surface of SnO_2 rather than remaining spread on it.

The conclusion of this series of experiments is that an artificial contamination as obtained by the impregnation of Mo ions on SnO_2 tends to spontaneously vanish. In other words, one must conclude that the tendency of MoO_3 and SnO_2 to get mutually contaminated through the coverage of their respective surfaces is very weak.

3.3. Role of the different types of mutual contamination between SnO_2 and MoO_3 in the dehydration–dehydrogenation of 2-butanol

3.3.1. Role of Sn–Mo–O mixed phase

The catalytic performances of mixed Sn–Mo–O oxide samples are presented in Table 3 as a function of the temperature of burning. The sample Sn–Mo–O/723 exhibited low conversion of 2-butanol and low yields in MEK and BUT. Sample Sn–Mo–O/823 presented the highest conversion and yields, while the sample Sn–Mo–O/973 gave intermediate values. The selectivity for BUT clearly increased when the burning temperature increased, i.e when the segregation of the Sn–Mo–O precursor to MoO_3 and SnO_2 increased. The highest selectivity to MEK was obtained for Sn–Mo–O/723 while this sample was less active and selective to BUT than pure MoO_3.

The fact that the selectivity to BUT increased significantly with the segregation of MoO_3 and SnO_2 from the Sn–Mo–O precursor suggests that the simultaneous presence of both simple oxides is important to increase the selectivity to BUT. The test performed with Sn–Mo–O/723, which should correspond to the highest level of mutual contamination between Sn and Mo for this series of samples, shows that this type of contamination, if it exists, could not explain the synergy observed when MoO_3 and SnO_2 were mixed mechanically. Indeed, Sn–Mo–O/723 exhibited a conversion and yields, in particular the yield in BUT, which were modest compared to those of the reference mechanical mixture of SnO_2 and MoO_3.

The high activity and selectivity in BUT observed for the sample Sn–Mo–O/823 are probably due to its higher specific surface area (24.2 $m^2\ g^{-1}$) than those of the other samples. SnO_2 and MoO_3 are segregated but most likely as small crystallites with numerous contacts between them. The large number of contacts between the simple oxides and the likely excellent quality of these contacts lead to an efficient cooperation between SnO_2 and MoO_3, so making the performance of Sn–Mo–O/823 high. As MoO_3 produces mainly BUT, this interpretation also accounts for the higher selectivity to BUT obtained with Sn–Mo–O/823 and Sn–Mo–O/973 in comparison with sample Sn–Mo–O/723. At the opposite, the higher selectivity to MEK observed for the sample Sn–Mo–O/723 is very likely explained by the fact that SnO_2,

Table 3
Catalytic performances of the mixed Sn–Mo–O samples and their mechanical mixtures with MoO_3 or SnO_2 in the dehydration–dehydrogenation of 2-butanol in the presence of oxygen

Catalysts	$\%C$	$\%Y_M$	$\%Y_B$	$\%S_M$	$\%S_B$
Sn–Mo–O/723	15.2	3.7	3.6	24.7	23.8
Sn–Mo–O/823	73.8	6.7	24.5	9.1	33.3
Sn–Mo–O/973	43.9	4.4	16.0	10.2	36.4
SnO_2	1.1	Traces	0.0	Traces	0.0
MoO_3	43.0	1.46	13.8	3.4	32.1
MoO_3 (50 wt.%) + SnO_2 (50 wt.%)	45.2	3.4	14.6	7.5	32.4
Sn–Mo–O/723 (10 wt.%) + MoO_3 (90 wt.%)	47.8	1.8	16.5	3.8	34.6
Sn–Mo–O/723 (90 wt.%) + SnO_2 (10 wt.%)	8.3	5.0	0.9	60.3	10.6

The conversion of 2-butanol ($\%C$) , the yields in BUT ($\%Y_B$) and in MEK ($\%Y_M$) and the corresponding selectivites ($\%S_B$ and $\%S_M$) are given. Values obtained for pure SnO_2, pure MoO_3 and their mechanical mixture are also presented.

which can only produce MEK because it does not possess the Brönsted acid sites required to produce BUT, is the only crystalline phase in the sample and by the low conversion and yield in MEK observed. The fact that the sample Sn–Mo–O/973 presented performances very similar to those of the reference mechanical mixture of SnO_2 and MoO_3 seems totally consistent with the above interpretation, as in Sn–Mo–O/973 the two metals have completely segregated from the amorphous precursor to form a mixture of pure simple oxides crystallites, as shown by the XRD.

Next to these aspects, Sn–Mo–O/723 sample has been used to study the catalytic influence that a mixed Sn–Mo–O contamination phase could exert on SnO_2 and/or MoO_3 after having possibly formed during the catalytic reaction from the initial mechanical mixture of pure simple oxides. The sample Sn–Mo–O/723 was therefore mixed with MoO_3 or SnO_2. The mixtures, respectively contained 90 wt.% of MoO_3 for 10 wt.% of Sn–Mo–O/723, and 10 wt.% of SnO_2 for 90 wt.% of Sn–Mo–O/723. Catalytic performances are presented in Table 3. Catalytic performances of Sn–Mo–O/723 mixed with MoO_3 were close to the mass-averaged addition of the activities obtained with pure Sn–Mo–O/723 and pure MoO_3. No synergy between the two compounds was thus observed in the formation of BUT nor in the selectivity to BUT. For the mixture of Sn–Mo–O/723 with SnO_2, the yield and the selectivity to MEK were enhanced with respect to the pure compounds. The conclusion of these experiments is that the mixed contaminated Sn–Mo–O phase is weakly active and mostly non selective and that it cannot induce a significant synergetic improvement of the performances of SnO_2 and MoO_3. Hence, it must be concluded that the only possible presence of such a Sn–Mo–O contamination could not induce an increase in the selectivity in BUT as that observed through the synergetic effects detected with the mechanical mixture of SnO_2 and MoO_3.

3.3.2. Role of Mo ions impregnated on SnO_2

$Sn_iMo(X)$ samples were used to study the influence of the concentration of Mo ions impregnated on the surface of SnO_2 on the catalytic performance of the system SnO_2–MoO_3. The results are presented in Table 4. Conversion, yields in MEK and BUT and, selectivity to BUT globally increase when the amount of Mo ions impregnated increases. Simultaneously, selectivity in MEK tends to decrease.

Table 4
Catalytic performance of $Sn_iMo(X)$ samples in the dehydration–dehydrogenation of 2-butanol in the presence of oxygen

Catalysts	$\%C$	$\%Y_M$	$\%Y_B$	$\%S_M$	$\%S_B$
$Sn_iMo(0.25)$	8.1	5.7	0	70.2	0
$Sn_iMo(0.5)$	12.6	9.2	0.9	73.1	7.3
$Sn_iMo(0.75)$	31.7	8.1	1.75	25.4	5.5
$Sn_iMo(1)$	56.1	20.2	11.9	21.3	21.2
$Sn_iMo(2)$	26.6	9.0	4.8	34.0	18.2

Conversion of 2-butanol ($\%C$), yields in BUT ($\%Y_B$) and MEK ($\%Y_M$) and the corresponding selectivities ($\%S_B$ and $\%S_M$) are given for Mo ions impregnated in different concentrations on SnO_2.

Taking into account the characterization results presented before which showed that the contamination tends to decrease as the amount of Mo impregnated increases (as MoO_3 tends to detach from SnO_2 to form independent crystallites), it can be concluded that the increase in the catalytic performances when the number of theoretical monolayers of Mo on SnO_2 increases must be attributed to the simultaneous presence of SnO_2 and of the crystallites of MoO_3 formed on its surface, with good contacts between them. Two additional justifications are necessary. First, when the amount of Mo ions becomes high, the catalytic performances decrease. This is observed when comparing the performances of $Sn_iMo(1)$ with those of $Sn_iMo(2)$. This can be explained by the fact that the size of the crystallites of MoO_3 increases when the amount of Mo ions impregnated increases, i.e. when the amount of Mo available to grow bigger MoO_3 particles increases. Correspondingly, the exposed area of MoO_3 decreases, which leads to the lower performance observed. Second, for the samples with low concentrations of Mo, the selectivity in MEK was high. This result certainly needs further investigation. At this stage of our research, a possible explanation could be that SnO_2 promotes a very efficient formation of MEK on very small crystallites of MoO_3 present at its surface. But, one does not have any decisive argument to discard the possibility that a minute contamination associating Sn and Mo, of a way still to discover, promotes selectively the formation of MEK. In any case, this result must certainly be considered together with the performance of the sample Sn–Mo–O/723 which similarly also gave a relatively high selectivity to MEK.

Table 5
Catalytic performances in the dehydration–dehydrogenation of 2-butanol in the presence of oxygen obtained for the mechanical mixtures of $Sn_iMo(0.5)$ with SnO_2 and MoO_3

Catalysts	$\%C$	$\%Y_M$	$\%Y_B$	$\%S_M$	$\%S_B$
$Sn_iMo(0.5)$ (50 wt.%) + MoO_3 (50 wt.%)	41.8	3.1	12.8	7.3	30.7
$Sn_iMo(0.5)$ (50 wt.%) + SnO_2 (50 wt.%)	6.2	3.9	0	62.9	0

Conversion of 2-butanol ($\%C$), yields in BUT ($\%Y_B$) and MEK ($\%Y_M$) and the corresponding selectivites ($\%S_B$ and $\%S_M$) are given.

The catalytic performance obtained for the mechanical mixtures of the $Sn_iMo(0.5)$ sample with SnO_2 and MoO_3 are presented in Table 5. The performance of the mixture of $Sn_iMo(0.5)$ and MoO_3 are almost identical to those obtained with the comparable mixture containing 50 wt.% of MoO_3 and 50 wt.% of SnO_2. For the mixture of $Sn_iMo(0.5)$ and SnO_2, the performance obtained were similar or lower than the performance expected if the two compounds behave without any cooperation between them. In particular, no BUT formation was detected in the case of the mixture.

From these results, it must thus be concluded that the presence of the superficial contamination of SnO_2 with Mo ions cannot account, either direcly or through a cooperation with simple oxides, for the synergetic improvements of the performance, in particular the formation of BUT as detected for the mechanical mixture of MoO_3 and SnO_2.

3.3.3. Role of the solid solution of Mo in SnO_2

As mentioned in the introduction, it is speculated that a solid solution of Mo in SnO_2 could form from a thin MoO_3 layer deposited on SnO_2 under the typical conditions chosen to run the dehydration–dehydrogenation of 2-butanol. For that purpose, the sample $Sn_iMo(0.5)$ was thus used in the 2-butanol reaction under the standard conditions, but during 4 h. It was thereafter tested again, as such and in mechanical mixtures with SnO_2 and MoO_3. The catalytic performances obtained with these samples as catalysts are presented in Table 6.

The sample $Sn_iMo(0.5)$ (treated) presented performance essentially similar to the sample $Sn_iMo(0.5)$. Particularly, the formation of BUT was not significantly improved after that the sample was submitted a first time to the 2-butanol reaction, and it led to a level of selectivity to BUT much lower than that obtained with the mechanical mixture of SnO_2 and MoO_3. Concerning the mechanical mixtures of $Sn_iMo(0.5)$ (treated) with SnO_2 and MoO_3, the performances obtained were in the range (or lower) of those obtained with the corresponding mixtures associating the simple oxides with the sample $Sn_iMo(0.5)$.

3.3.4. Summary

The series of experiments described above showed that (i) none of the three types of contamination investigated in this work used as such in the dehydration–dehydrogenation of 2-butanol in the presence of oxygen exhibits catalytic performance susceptible to account for the synergetic effect observed for mechanical mixtures of SnO_2 and MoO_3, and (ii) the mechanical mixtures of the different contamination compounds with SnO_2 and MoO_3 present similar performances to those obtained with the mixtures of non contaminated simple oxides. The conclusion is thus that the contamination of one of the oxides by the

Table 6
Catalytic performances obtained for the $Sn_iMo(0.5)$ (treated) sample and its mechanical mixtures with SnO_2 and MoO_3 in the dehydration–dehydrogenation of 2-butanol in the presence of oxygen

Catalysts	$\%C$	$\%Y_M$	$\%Y_B$	$\%S_M$	$\%S_B$
$Sn_iMo(0.5)$ (treated)	19.5	10.9	0.4	56	2.1
$Sn_iMo(0.5)$ (50 wt.%) (treated) + MoO_3 (50 wt.%)	34.9	2.9	12.9	8.5	37.2
$Sn_iMo(0.5)$ (50 wt.%) (treated) + SnO_2 (50 wt.%)	5.8	4.5	0	77.4	0

Conversion of 2-butanol ($\%C$), yields in BUT ($\%Y_B$) and MEK ($\%Y_M$) and the corresponding selectivites ($\%S_B$ and $\%S_M$) are given.

element coming from the other, and a new mixed oxide phase associating both metals, if they exist and remain stable under the conditions of reaction, do not play any significant role in the synergetic effects observed between MoO_3 and SnO_2 mixtures during the dehydration–dehydrogenation of 2-butanol at low temperature, this neither by their own activity nor by developing a cooperation with the pure oxides. The hypothesis that SnO_2 controls at distance, through a remote control mechanism via the migration of Oso, the activity of MoO_3 as an external phase, i.e. remaining completely independent from MoO_3, is thus further supported by the investigation presented in this paper. The role played by Oso during the conditions of catalysis has been further investigated by studying the acidity of oxides and mixtures as described in the next sections.

3.4. Investigation of the Brönsted acidity of MoO_3 in the presence of SnO_2

NH_3-TPD experiments were realized with pure MoO_3(I), SnO_2(I) and their mechanical mixtures containing 25, 50, 75 and 90 wt.% of Mo oxide. Results are presented in Fig. 1. The spectra representing the amount of NH_3 desorbed as a function of the temperature, have been divided arbitrary into three ranges of desorption temperature. These ranges correspond to the desorption of NH_3 from acid sites with different strengths. The different acid site strengths were referred to weak sites for the NH_3 desorption proceeding between 343 and 423 K, medium sites for the NH_3 desorption proceeding between 423 and 523 K, and strong sites for the NH_3 desorption proceeding between 523 and 723 K. The amount of NH_3 desorbed for each range of temperature is thus directly proportional to the amount of acid sites of each acidity strength present at the surface of the analyzed sample.

No acid sites were detected for pure SnO_2. Pure MoO_3 presented few amounts of acid sites with weak and strong strengths, but a significant amount of medium acid sites. The number of acid sites detected for the mechanical mixtures were systematically more important than for the pure oxides. The effect was particularly obvious for the weak and medium acid sites.

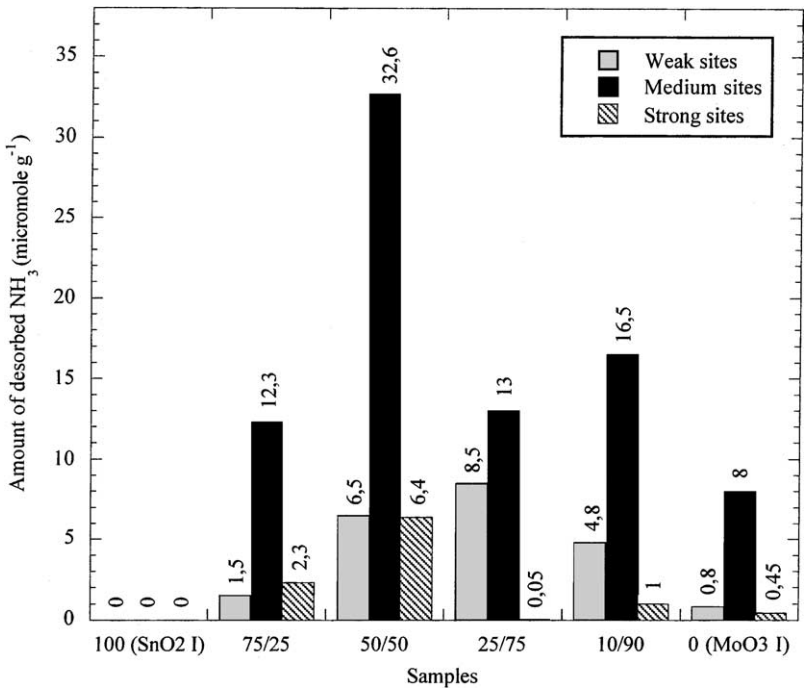

Fig. 1. TPD results for pure MoO_3(I), pure SnO_2(I) and their mechanical mixtures. The ranges of acidity strength are defined in the text. Acidity is expressed in terms of amount of NH_3 desorbed from the samples.

The experiment shows that the only fact of mixing mechanically MoO_3 with SnO_2 induces a significant increase of the acidity of the system. It is interesting to note that this conclusion was also previously reached when studying mixtures of MoO_3 with α-Sb_2O_4 [11]. In this case, the dehydration of *N*-ethyl-formamide to propionitrile, an oxygen-aided reaction which proceeds on Brönsted acid sites, was used as the probe reaction. A remarkable increase in the dehydration performance was observed when MoO_3 was used in mixture with α-Sb_2O_4. For the mixtures, a strong linear correlation was found between the amount of NH_3 desorbed from Brönsted sites and the propionitrile yield. It was moreover shown that α-Sb_2O_4 is an efficient Oso donor [21]. The increase in acidity was thus explained by the remote control mechanism, namely the formation of Oso at the surface of α-Sb_2O_4, the migration of Oso onto the surface of MoO_3 followed by its reaction with it. The creation of Oso on Oso donor phases has already been extensively described and discussed elsewhere [3]. In the case of α-Sb_2O_4, the most plausible scheme for the formation of Oso is based on the existence in the structure of the oxide of oxygen ions making a bridge between a Sb^{5+} ion and a Sb^{3+} ion. These oxygen ions are highly polarizable which confers them a strong tendency to leave the structure, so forming at the surface monoatomic nucleophilic oxygen species, namely Oso. A consequence of the formation of Oso is the reduction of the Sb^{5+} ion to an additional Sb^{3+} ion. Under the conditions of the catalytic reaction, namely in the presence of molecular oxygen, a second step is the reoxidation of the reduced Sb^{3+} ion to the +5 oxidation state. At that stage, α-Sb_2O_4 has recovered its initial structure and can undergo another cycle of Oso formation. During the TPD of NH_3, the reoxidation of the antimony oxide does not happen as none of the steps of the experiment are carried out with a presence of O_2 in the gas feed. However, the first step of the Oso formation cycle may proceed as under the conditions of catalysis, so generating the flow of Oso in the system, in particular its migration onto the surface of MoO_3.

The mechanism proposed to account for the ability of Oso to induce the creation of acid sites on MoO_3 is based on the tendency of Oso to share electrons with surface Mo^{6+} ions. This phenomenon leads to a partial compensation of the polarization of the lattice oxygen atoms surrounding Mo atoms, which tends to render Mo positively charged. This effect results in an increase of the density of negative charges on the unsaturated oxygen atoms, so increasing the possibility of these of adsorbing a proton, in other words, so increasing the number of Brönsted acid sites on MoO_3. During the TPD experiment, the adsorption of NH_3 at the surface of MoO_3 is thus favored when Oso is present in the system, namely when α-Sb_2O_4 is mixed with MoO_3.

One has to remind that since this interpretation was given, the tendency of MoO_3 to undergo a reconstruction of its crystals in the presence of Oso and to stabilize in a suboxide stoichiometry was discovered [6–8]. Another hypothesis to account for the increase of the Brönsted acidity of MoO_3 through the remote control mechanism could thus simply be that the reconstructed MoO_3 or the Mo suboxides possess more acid sites for reasons coming from their crystallographic peculiarities. This hypothesis still needs to be further investigated. In the case it should prove to be valid, it must be understood as concerning an additional mechanism of acid site creation induced by Oso, namely in addition to the mechanism described in the previous paragraph, rather than an alternative one. It is not yet fully ascertained whether the creation of acid sites by reconstruction of MoO_3 to a suboxide could proceed during the conditions of the TPD experiment.

Our interpretation of the data reported in this work in the case of the mixtures of SnO_2 and MoO_3, in particular the synergetically improved formation of BUT, is that when MoO_3 is mixed with SnO_2, an identical phenomenon happens as when MoO_3 is mixed with α-Sb_2O_4. As it is already proven experimentally, SnO_2 is thus considered as a Oso donor phase while MoO_3 remains the Oso acceptor of the system [12]. Our experiments thus suggest that Oso formed on SnO_2 reacts with the surface of MoO_3 so creating more numerous acid sites. These sites are responsible of the increase in the yield and the selectivity of BUT measured when MoO_3 was in mixture with SnO_2. The mechanism of the formation of Oso by other Oso donors than α-Sb_2O_4, in particular by SnO_2, is discussed in [3].

3.5. Synergetic effects between SnO_2 and MoO_3 at high temperature

The investigation of the synergetic effects between SnO_2 and MoO_3 at high temperature was realized with

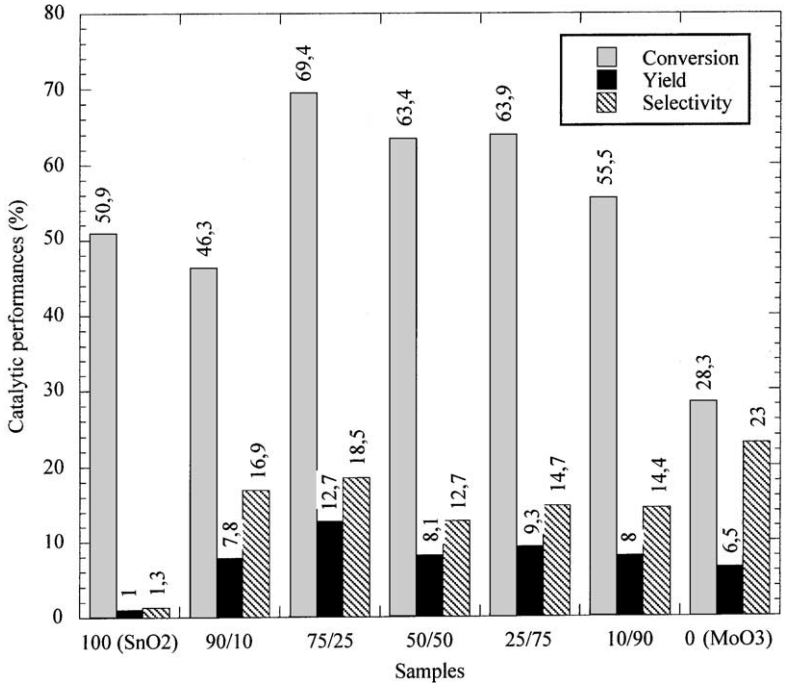

Fig. 2. Catalytic performances obtained for the mechanical mixtures of MoO_3(I), SnO_2(I) and their mechanical mixtures in the selective oxidation of isobutene to methacrolein. Conversion of isobutene, yield in methacrolein and selectivity to methacrolein are given.

the selective oxidation of isobutene to methacrolein. The catalysts were pure MoO_3(I), SnO_2(I) and their mechanical mixtures containing 10, 25, 50, 75 and 90 wt.% of Mo oxides. The performances measured at 693 K are presented in Fig. 2.

Pure SnO_2 is very active but almost not selective to methacrolein. Pure MoO_3 is less active but more selective. Significant synergetic effects were observed for the mixtures. For the mixture containing 25% of MoO_3, the conversion of isobutene had increased by about 104%, the yield in methacrolein by about 148% and the selectivity to methacrolein by about 256% with respect to the performances that would have been obtained if the phases had behaved completely independently (without any cooperation between them) during the reaction. The conclusion of this experiment is that the simultaneous presence MoO_3 and SnO_2 in the mechanical mixtures induces a synergetic effect at higher temperatures. This is consistent with the finding of a similar synergy between the two oxides in the oxidation of ethanol to acetic acid and acetaldehyde between 573 and 723 K, and in the oxidative dehydrogenation of methanol to formaldehyde [22,23].

Physico-chemical characterization by specific surface area measurements, XRD and XPS of the catalysts used in the oxidation of isobutene showed that pure MoO_3 and SnO_2 remained unchanged after the reaction. Contrary, in the case of the mixtures, MoO_3 got significantly reduced (Mo in the +4 oxidation state was observed at the surface of the samples) while SnO_2 remained unchanged. The extent of the reduction of MoO_3 depended on the composition of the mixture.

This series of experiments shows that at high temperature another phenomenon occurs in the system investigated here. It is the fact that SnO_2 promotes the reduction of MoO_3 during the reaction. The explanation resides probably in the fact that, at high temperature, SnO_2 is too active and tends to deeply oxidize isobutene. This leads to the creation of numerous oxygen vacancies at its surface. As most of the oxides of transition metals, pure SnO_2 is not able to completely regenerate by its own the reduced sites at its surface by using molecular oxygen. The data reported here suggest that the oxygen deficiency at the surface of SnO_2 is fulfilled through the diffusion

of lattice oxygen pumped from MoO_3. MoO_3 thus consequently got progressively reduced as it is not able to efficiently regenerate alone its own reduced sites by using O_2. It is interesting to remind that the identical phenomenon was observed in the oxidation of ethanol to acetic acid. In this last case, it was observed that the reduction of MoO_3 in the mixtures with SnO_2 was inhibited by the presence of α-Sb_2O_4 [18]. This last point reinforces the idea that the migration of Oso species plays a very important role in the control of the performances of this kind of catalytic systems.

4. Conclusion

1. Contamination of the surface of SnO_2 with Mo ions or the formation of a new Sn–Mo–O mixed phase cannot explain the synergetic effects observed in the mechanical mixture associating pure SnO_2 and MoO_3. The synergetic effects should thus be explained by a long distance action, precisely a remote control mechanism via the migration of Oso. This work shows that even at low temperature, SnO_2, which is mostly inactive in the dehydration–dehydrogenation of 2-butanol in the presence of oxygen, acts as Oso donor and so triggers the enhancement of the catalytic performance of MoO_3 which behaves as a Oso acceptor.
2. Oso increases the acidity of MoO_3. The phenomenon thus leads to an increase in the formation of BUT. Another effect of Oso is also to induce the regeneration of the dehydrogenation sites of MoO_3, likely by maintaining a high surface oxidation level of the superficial Mo atoms. The phenomenon leads to an increase in the formation of MEK.
3. The system SnO_2–MoO_3 works synergetically at high temperature in the oxidation of isobutene. However, under these conditions, SnO_2 is highly active and it got reduced continuously during reaction when used alone, so loosing activity and selectivity. In the presence of MoO_3, SnO_2 pumps lattice oxygen from the Mo oxide lattice. The phenomenon leads to the stabilization of the performance of SnO_2 but also to the reduction of MoO_3.

5. Outlook

Several investigations have been conducted in our laboratory in order to study synergetic effects in biphasic catalysts in the oxidation of hydrocarbons [3]. Our studies show that one of the reasons of the synergetic effects detected in multiphase catalysts is the presence of phases acting as activator of Oso species. In these studies, we carefully took into account alternative explanations of the cooperation observed, in particular, the possible formations of mutual contamination or of new mixed oxide compounds. Our results led to a classification of the oxides used in multiphase catalysts on a donor of Oso—acceptor of Oso scale. Typically α-Sb_2O_4 appears on the scale as a strong donor of Oso while MoO_3 appears as an acceptor of Oso. Many oxides have a dual role depending on the conditions of reaction and on the other phases in the presence of which they are used as catalysts. This is the case of Bi_2MoO_6 in the oxidation of isobutene to methacrolein. SnO_2 also plays a dual role as observed during the dehydratation-dehydrogenation of 2-butanol in the presence of oxygen. SnO_2 behaves as an acceptor in the presence of α-Sb_2O_4 but as a donor in the presence of MoO_3. An important point to mention on the present work is that the results show that the migration of Oso and the remote control mechanism can also operate at low temperatures, while until now they were globally only evoked when temperatures above 673 K were concerned. This work clearly supports our previous interpretation obtained in the frame of catalytic reactions run at high temperatures, and also opens new perspectives for the understanding of the catalytic mechanisms occurring in multiphase oxidation catalysts.

Acknowledgements

The financial supports from the Région Wallonne (Belgium) in the frame of an ‘‘Action Concertée’’ and from the DGICYT—Ministerio de Educación y Ciencia de España in the frame of a FPU program are gratefully acknowledged for the fellowship awarded to S.R.G. Carrazán and for the acquisition of several physico-chemical characterization equipments. The National Foundation for Scientific Research (FNRS) of Belgium is thanked for the position awarded to

E.M. Gaigneaux. The authors also thank M.J. Genet for his help in the XPS analyses, and L. Ghenne for her help in the syntheses described in this work.

References

[1] E.M. Gaigneaux, D. Herla, P. Tsiakaras, U. Roland, P. Ruiz, B. Delmon, ACS Symp. Ser. 638 (1996) 330.
[2] E.M. Gaigneaux, P. Tsiakaras, D. Herla, L. Ghenne, P. Ruiz, B. Delmon, Catal. Today 33 (1997) 151.
[3] L.-T. Weng, B. Delmon, Appl. Catal. A 81 (1992) 141.
[4] B. Delmon, Surf. Rev. Lett. 2 (1995) 25.
[5] B. Delmon, Heter. Chem. Rev. 1 (1994) 219.
[6] E.M. Gaigneaux, P. Ruiz, B. Delmon, Catal. Today 32 (1996) 37.
[7] E.M. Gaigneaux, P. Ruiz, E.E. Wolf, B. Delmon, Appl. Catal. 121/122 (1997) 552.
[8] E.M. Gaigneaux, M.-L. Naeye, O. Dupont, M. Callant, B. Kartheuser, P. Ruiz, B. Delmon, DGMK Tagunsbericht 9803 (1998) 181.
[9] E.M. Gaigneaux, M.-L. Naeye, O. Dupont, P. Ruiz, B. Delmon, Shokubai 41 (1999) 82.
[10] E. Godard, E.M. Gaigneaux, P. Ruiz, B. Delmon, Catal. Today 61 (2000) 279.
[11] E.M. Gaigneaux, H.M. Abdeldayem, E. Godard, P. Ruiz, Appl. Catal. A 202 (2000) 265.
[12] B. Delmon, P. Ruiz, S.R.G. Carrazan, S. Korili, M.A. Vicente Rodriguez, Z. Sobalik, Stud. Surf. Sci. Catal. 100 (1996) 1.
[13] Ph. Courty, H. Ajot, Ch. Marcilly, B. Delmon, Powder Technol. 7 (1973) 21.
[14] Powder Diffraction File, Joint Committee on Powder Diffraction Standards, International Centre for Diffraction Data (JDPDC-ICDD). 1996: Cards 211250 and 050508.
[15] J. Sonnemans, P. Mars, J. Catal. 31 (1973) 209.
[16] C. Defossé, J. Electron Spectrosc. Relat. Phenom. 23 (1981) 157.
[17] R.F. Rielman, A. Msezane, S.T. Manson, J. Electron Spectrosc. Relat. Phenom. 8 (1976) 389.
[18] L.-T. Weng, G. Vereecke, M.J. Genet, P. Bertrand, W.E.E. Stone, Surf. Interf. Anal. 20 (1993) 179.
[19] J.H. Scofield, J. Electron Spectrosc. Relat. Phenom. 8 (1976) 129.
[20] J. Szajman, J. Liesegang, J.G. Kenkin, R.C.G. Leckey, J. Electron Spectrosc. Relat. Phenom. 23 (1981) 97.
[21] Z. Bing, T. Machej, P. Ruiz, B. Delmon, J. Catal. 132 (1991) 183.
[22] R. Castillo, P.A. Awasarkar, Ch. Papadopoulou, D. Acosta, P. Ruiz, B. Delmon, Stud. Surf. Sci. Catal. 82 (1994) 795.
[23] N.G. Valente, L.E. Cadus, O.F. Gorriz, L.A. Arrua, J.B. Rivarola, Appl. Catal. A 153 (1997) 119.